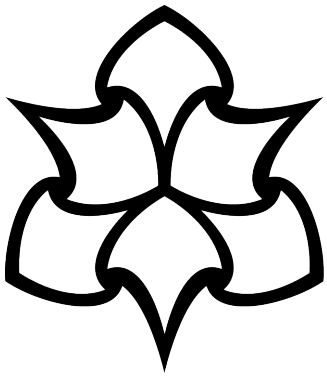

Assessment of microstructural changes in Grade 91 power station tubes through permeability and magnetic Barkhausen noise measurements

John W. WILSON [1], Jun LIU [2], Noushin KARIMIAN [1], Claire L. DAVIS [2], Anthony J. PEYTON [1]

[1] School of Electrical and Electronic Engineering, University of Manchester, Manchester M13 9PL, UK
Phone: +44 161 3068716, e-mail: john.wilson@manchester.ac.uk
[2] School of Metallurgy and Materials, University of Birmingham, Edgbaston, Birmingham B15 2TT, UK

Abstract
The use of Grade 91 steel for high-temperature power plant applications can result in substantial reductions in component thickness compared to weaker alloys, resulting in reduced thermal stresses and improved service life. Although Grade 91 offers superior resistance to thermal fatigue and creep to other grades used in the industry, this is dependent on the creation and maintenance of a specific microstructure, which can be altered through routine component fabrication, installation and maintenance. Electromagnetic inspection has the potential to assess the level of degradation in steel components through in-situ measurements. In this work, correlations are drawn between microstructural changes in heat treated Grade 91 samples and electromagnetic properties including incremental and differential permeability and Barkhausen noise. These correlations are first established by examining machined samples using a closed magnetic loop, lab-based system, and then transferred to open magnetic loop measurement of tube samples. The results demonstrate the potential viability of electromagnetic methods for inspection of power station tubes in-situ.

Keywords: Electromagnetic, steel, Barkhausen noise, permeability, hysteresis

1. Introduction

The introduction of the modified 9Cr-1Mo alloy; Grade 91 ("P91" for piping and "T91" for tubing), for high-temperature applications can result in substantial reductions in component thickness compared to weaker alloys, such as Grade 22. The thinner wall produces substantially reduced thermal stresses and thereby improves service life [1]. Grade 91 steel is produced by heating 9Cr-1Mo material to approximately 38 ºC above its upper critical transformation temperature (AC3) until fully austenitic. The steel is then cooled in air to below 204 ºC, at which point the austenite is fully transformed into untempered martensite. This normalising process produces a structure that is very strong, but brittle. The material is then tempered at around 760 ºC to improve ductility and toughness, and to induce the formation of critical carbide and carbo-nitride precipitates [1].

Although Grade 91 offers superior resistance to thermal fatigue and creep damage, which occurs in components exposed to high pressures and high temperatures, this is dependent on the creation and maintenance of a tempered martensite microstructure for optimum performance. This microstructure can be altered through routine component fabrication, installation and maintenance procedures such as hot bending, forging and welding, so it is vital that NDE procedures are developed which can monitor these changes.

Current procedures for the assessment of microstructural changes in components in power stations involve site inspections during shut-down periods and inspection of steel components often involves procedures such as replica metallography [2, 3] or hardness testing. The use of electromagnetic (EM) sensors for inspection has the potential to provide information on microstructural changes in steel by exploiting the link between the microstructure and magnetic domain structure of the material. EM inspection [4-6] has the advantage that it can be performed in-situ, at elevated temperatures, with minimal surface preparation. EM properties are however highly material and microstructure specific, so inspection techniques

must be calibrated to particular materials and tailored to monitor known microstructural changes, if these techniques are to be deployed with confidence.

A number of different approaches are available to assess the magnetic properties of a particular material; the most basic of these is the measurement of the major BH loop [7]. Values derived from the major loop, such as coercivity, permeability and hysteresis loss, can be used to quantify the magnetic hardness of a material, which in turn is indicative of material hardness [8, 9]. In addition to these major loop properties, information can also be derived from small minor loop deviations from the major loop or initial magnetisation curve.

Although these techniques both involve the measurement of flux density B in response to an applied field H, the interaction between magnetic domains and material microstructure can be different as the microstructural features effectively pinning domain walls vary with the applied field strength. The major loop response consists of a combination of reversible and irreversible effects [10]; irreversible magnetisation from domain walls overcoming pinning sites such as inclusions, dislocations and grain boundaries and reversible magnetisation from domain wall motion and rotation of magnetic domains. In contrast, the minor loop response to a very small applied field is predominantly reversible; corresponding to bowing of domain walls around pinning sites and domain rotation at higher major loop offsets [10,11]. Previous work [12] has shown that minor loop parameters show greater sensitivity to changes in material properties such as hardness; this has been attributed to the technique's high sensitivity to lattice defects.

Although the link between magnetic Barkhausen noise (MBN) activity and material properties such as hardness and residual stress is more complex, using techniques such as analysis of the MBN profile [6, 13], a more comprehensive understanding of the magnetic domain structure of the material can be developed. Through this deeper understanding of the domain structure, information pertaining to the material microstructure can be inferred through the interaction between domain walls and lattice defects such as dislocations, grain boundaries, impurity atoms and precipitates [14]. As these microstructural changes are major causes of degradation for power station steels, MBN could be a useful tool for the quantification of this degradation, when used in conjunction with other techniques. Although some success has been achieved using magnetic methods for the inspection of Grade 91 steel [8], these methods must be adapted for the inspection of pipes and tubes in service, rather than prepared samples.

In this paper, magnetic measurements including major BH loop measurements, incremental permeability derived from minor BH loops and analysis of the MBN profile are used to measure the magnetic properties of Grade 91 steel samples. Two sets of samples are inspected with two different inspection systems; cylindrical machined samples are inspected using a closed magnetic loop, lab based system and sections of tube are inspected using an open magnetic loop system and the results from the two systems compared.

2. Measurement System and Sample Summary

2.1 Measurement system

A schematic of the measurement system developed for the tests is shown in Figure 1. A low frequency time varying signal is fed to two power amplifiers, which supply current to two excitation coils wrapped around a silicon-steel core. The cylindrical sample to be tested is fitted into a slot in the core, to maximise coupling between core and sample. The axial applied field (H) is measured using a Quantum Well Hall sensor, developed at the University of

Manchester [15]. The flux density of the induced field (B) is measured using a 20-turn encircling coil connected to an instrumentation amplifier. For MBN measurements, the 20-turn coil is replaced with a 6000-turn encircling coil and the low frequency component of the signal is rejected through the addition of a passive 5 kHz high-pass filter.

For the major loops, a 1 Hz sinusoidal excitation is used and 9 cycles are recorded and averaged. A 10 Hz sinusoidal excitation is used to generate the minor loops, with two types of minor loop being recorded:

1) Logarithmic amplitude sweep. The sample is demagnetised by the application of 10 Hz sinusoidal excitation, gradually reducing in amplitude. The applied field is then increased to a pre-determined amplitude and several minor loop cycles recorded. This is repeated several times, with the loop amplitude increasing logarithmically.
2) Deviations from the main B-H loop. In this case, the sample is taken through several major loop cycles before the applied field is held constant at a pre-determined H value and several minor loop cycles are recorded.

For both types of minor loop, up to 90 cycles are acquired and averaged, to reduce noise.

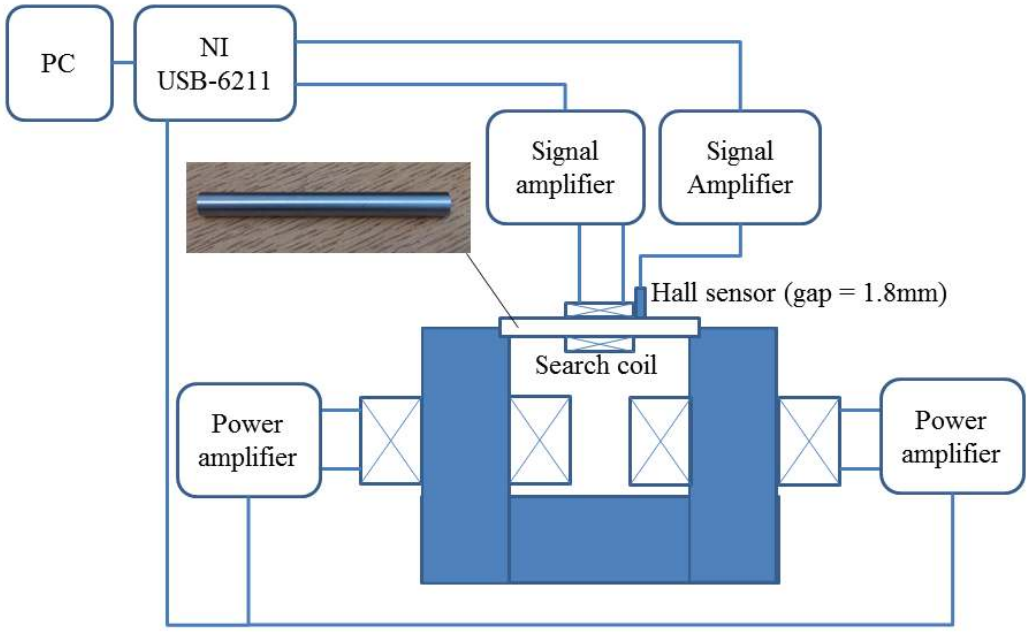

Figure 1. Schematic of lab-based measurement apparatus

The 1 Hz sinusoidal excitation is used to generate major loop MBN profiles, with the signal from the MBN pickup coil and the applied axial field from the Hall sensor being recorded simultaneously. The signal from the coil is then high-pass filtered at a frequency of 5 kHz, rectified, and a moving average technique used to generate the MBN profile, which is then plotted against H.

The test system used for the tube samples (Figure 2) is an adaptation of the lab-based system shown in Figure 1. Excitation is provided by a U-core, contoured to the profile of the tube. The excitation system is similar to that shown in Figure 1; in this case the U-core is wrapped with two 160-turn excitation coils. H measurement is accomplished using a Quantum Well Hall sensor positioned 1.5 mm from the sample surface. B measurement is via a 10-turn coil, encircling the leg of the excitation yoke. The signal conditioning system and signal processing techniques are similar to those detailed for the lab-based system.

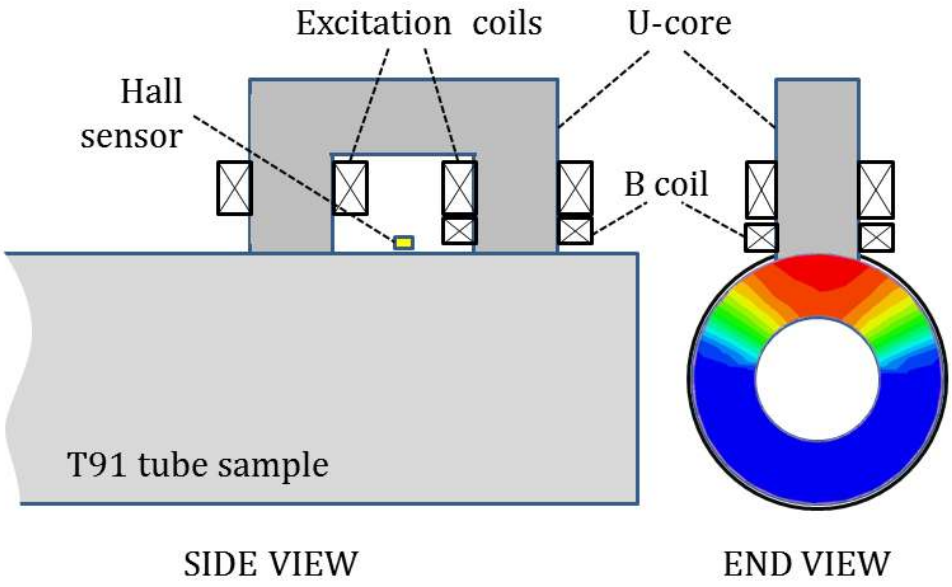

Figure 2. Schematic of measurement system for tube samples

2.2 Test samples

T91 steel tubes (53 mm outer diameter, 13.5 mm wall thickness and > 900 mm length) were supplied by the Electrical Power Research Institute (EPRI) as normalised at 1060 °C for 20 minutes and tempered at 780 °C for 1 hour. The chemical composition of the steel is given in Table 1. Cylindrical samples (4.95 mm diameter and 100 mm length) were machined from the tube for EM measurements using the BH loop measurement system described earlier. Selected cylindrical samples have been heat treated to different conditions in laboratory furnaces to simulate the microstructures expected from prolonged thermal exposure by accelerated tempering at 780 °C for 100 hours or mis-heat treatments / mis-manufacturing. The accelerated tempering condition was chosen because it generated significant microstructural degradation. The mis-heat-treatment was simulated by the following procedure [16] in order to generate a partially ferritic structure rather than a fully martensitic one on air cooling:

1. Heating up to 950 °C and dwelling for 30 min;
2. Programmed furnace cooling by 100 °C/h down to 760 °C;
3. Dwelling for 3 h;
4. Cooling in still air.

These heat treatments were carried out on two 250mm lengths of Grade 91 tube and cylindrical samples (4.95 mm diameter and 100 mm length) machined from the tube for closed loop EM measurements. This process resulted in the following samples:

- T91-AR: As received (service entry) condition. The Vickers hardness (HV) = 237 ± 2.1. Tempered martensite consisting of martensitic laths with many precipitates (mainly $M_{23}C_6$) on the lath boundaries (cylinder and tube samples)
- T91-T100h: Tempered at 780 °C for 100 hours. HV = 195 ± 2.2. Laths and precipitates significantly coarsened and equi-axed sub-grains had developed. Significant degeneration of the tempered martensite, comparable with degeneration due to prolonged service exposure (cylinder and tube samples)
- T91-M: Simulated mis-heat treatment. HV = 157 ± 3.5. Ferritic microstructure consisting of equi-axed ferrite grains, with a high number density of coarse

precipitates occurring on ferrite grain boundaries and many coarse and fine precipitates within the grains (cylinder and tube samples).

One further cylindrical sample, T91-ES (4.95 mm diameter and 50 mm length), was machined from an ex-service section of tube; 44.5 mm outer diameter, 6.3 mm wall thickness and < 70 mm length that had been taken from service as an antler tube on a superheater outlet header at 585 °C, under 16.5 MPa pressure (designed) for about 50,000 hours. The tube has a microstructure of slightly degenerated martensite with slightly increased lath size as compared to the T91-AR sample, with some equi-axed subgrains. Few precipitates within the laths or grains were observed.

Table 1. Chemical composition (weight percent) of the as-received T91 tube material

C	Si	Mn	P	S	Cr	Mo	Ni	V	Nb	N	Ti
0.11	0.271	0.469	0.015	0.003	8.9	1.00	0.135	0.169	0.055	0.046	0.003

As all samples have been tempered as received, they are thought to be free from significant residual stress, which may skew the EM response. Although there may be some residual stress within the ex-service tube due to pressure in service, this will have been substantially reduced through the machining process. Full metallurgical details of the samples with micrographs can be found here [17].

2. Measurements and experimental results

2.1 Major BH loop measurements

Figure 3 shows major BH loops for the cylindrical samples (Figure 3a) and the tube samples (Figure 3b). The change in shape of the BH loops for the cylindrical samples for 100 hour tempering (T91-T100h) as compared to the as received sample (T91-AR) follows the same trend observed by Piotrowski et al. [9]. The loop becomes thinner, with a corresponding decrease in coercivity (see Table 2) and an increase in 'squareness' leading to an increase in remanence. The mis-heat treated sample exhibits a further decrease in coercivity in-line with the further decrease in hardness.

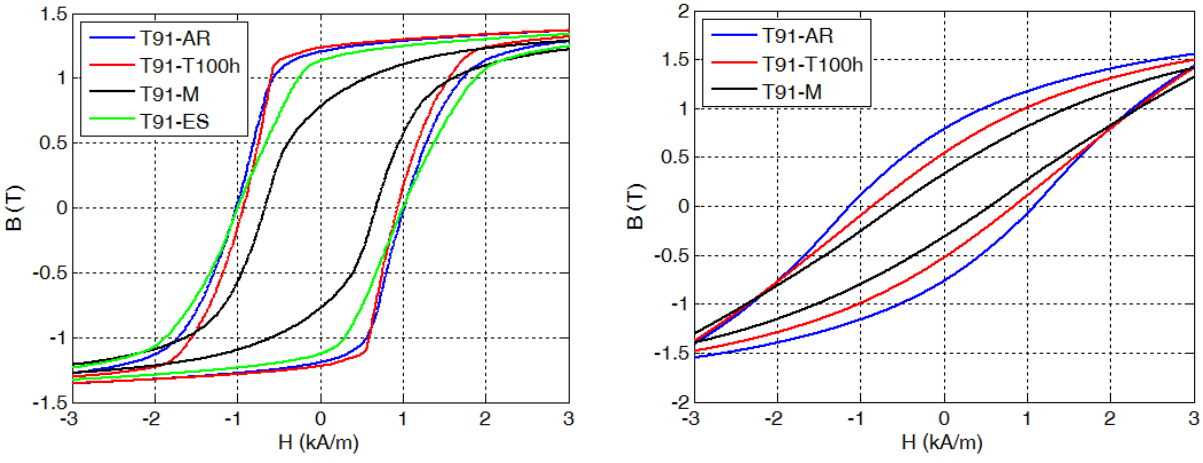

(a) **(b)**

Figure 3. a) Major BH loops for cylindrical samples, b) Loops for tube samples

The decrease in coercivity with decreasing hardness can also be observed in the loops for the tube samples (Figure 3b), although the shape of the loops is different due to the indirect measurement of B using a coil wrapped around the core, rather than around the sample; the latter is not practical for open samples. Although there are geometrical influences on the measurement of the H field, clearly the measured H values are more reliable than the measured B values in this system, so as long as the point at which B=0 can be identified, and the material can be driven reasonably close to saturation, reliable coercivity measurements can be made.

2.2 Incremental permeability and MBN

Figure 4 shows incremental permeability curves for the cylinder (Figure 4a) and tube (Figure 4b) samples. The curves are derived from logarithmic amplitude sweeps with the incremental permeability values calculated as the ratio between the change in B and the change in H ($\mu = \Delta B / \Delta H$). It can be seen from the plots that the curves for the cylinders and the tubes follow the same general trend, especially at lower loop amplitudes, with the magnetically and mechanically softest sample (T91-M) having the highest permeability at low loop amplitudes and the hardest sample (T91-AR) having the lowest permeability at low loop amplitudes. Polynomial fitting has been used to extrapolate initial permeability (μ_i) values for the samples, corresponding to the permeability value that would be reached if H = 0. These values are shown in Table 2.

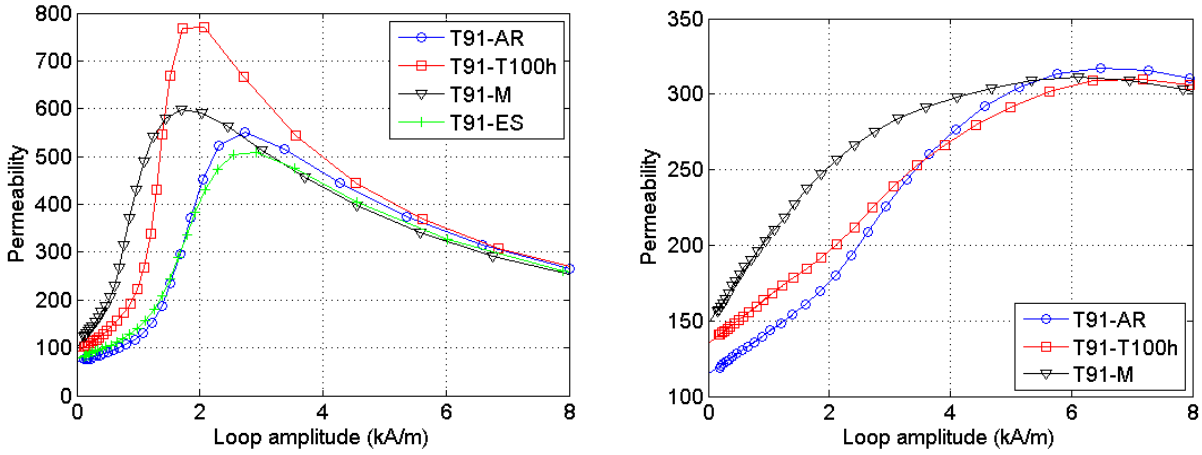

Figure 4. Incremental permeability derived from logarithmic amplitude sweep for; a) Cylindrical samples, b) Tube samples

Figure 5 shows magnetic Barkhausen noise profiles and incremental permeability curves for the cylindrical samples. Sinusoidal excitation, (frequency 1 Hz) is used to generate the MBN profiles, with the signal from the MBN pickup coil and the applied axial field from the Hall sensor recorded simultaneously. The signal from the coil is then high-pass filtered at a frequency of 5 kHz, rectified, and a moving average technique used to generate the MBN profile, which is then plotted against H. The incremental permeability (μ_Δ) curves are generated by superimposing small amplitude minor loops on major BH loops and calculating the resultant permeability values. The minor loop amplitude is then increased from 170 A/m to 850 A/m. Only the permeability curves from the increasing half of the major BH loop are shown.

It can be seen from Figures 5a and 5b that the peaks in the MBN profiles and μ_Δ curves shift to a lower H value for the softer T91-M sample. This is expected as the softer sample is easier to magnetise, therefore both MBN and (μ_Δ) reach a maximum at a lower applied field. The results for the tempered sample (Figure 5c) are more complex, as the MBN profiles exhibit two distinct peaks. This phenomena has previously been observed in as-tempered (at 750˚C) P9 steels, as well as T22 and 0.2 wt% carbon steels, [13] with peak 1, at a lower applied field being attributed to irreversible movement of domain walls at ferrite lath/grain boundaries and peak 2, at a higher applied field being attributed to irreversible movement of domain walls overcoming resistance offered by carbide precipitates. It is interesting to note that the first peak only appears in the incremental permeability profiles at higher minor loop amplitudes, indicating that greater energy is required to overcome domain wall pinning at ferrite lath/grain boundaries.

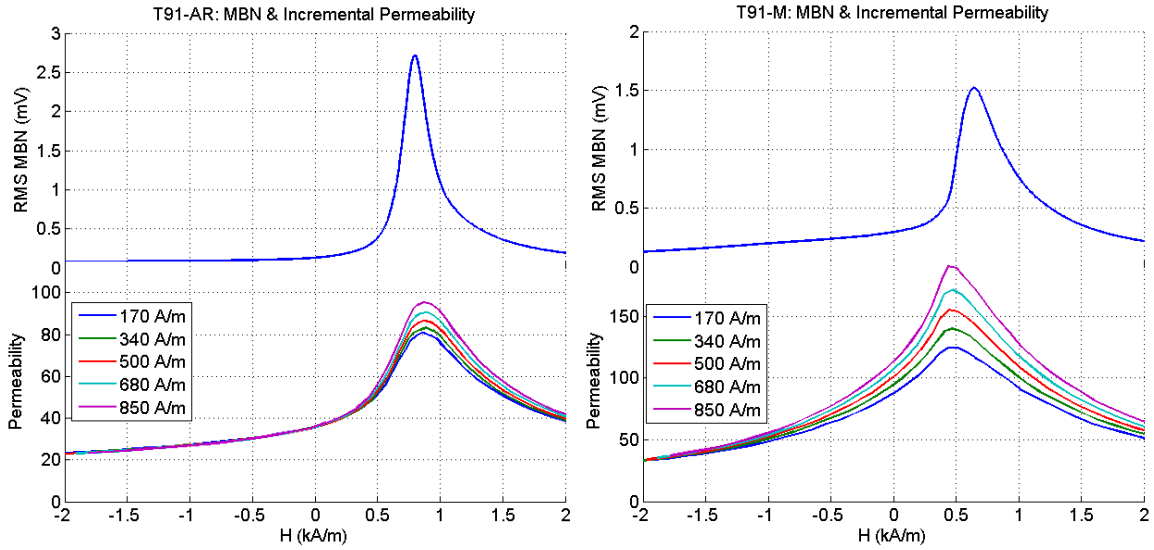

(a)

(b)

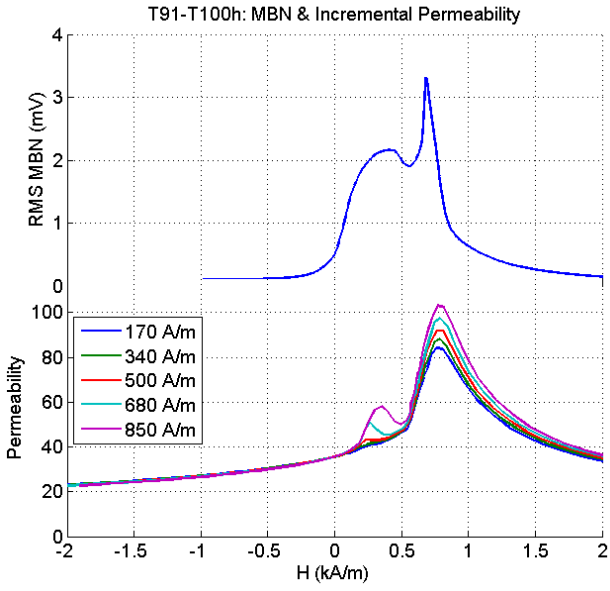

(c)

Figure 5. a) MBN profiles and incremental permeability derived from major BH loop for cylindrical samples

3. Discussion and Conclusions

In this paper, results from two EM measurement systems have been presented and compared. The closed magnetic loop, lab based system has been used to establish relationships between EM signal features including coercivity, initial permeability and MBN profile peak position and material properties such as Vickers hardness. The open magnetic loop deployable system was then used on heat treated tube samples to ascertain if these relationships could be used to develop a system that could be used on Grade 91 power station tubes in-service.

Table 2. Vickers hardness, coercivity and initial permeability of cylinder and tube samples

	Cylinder				Tube		
	T91-AR	**T91-T100h**	**T91-M**	**T91-ES**	**T91-AR**	**T91-T100h**	**T91-M**
HV	237 ± 2.1	195 ± 2.2	157 ± 3.5	219 ± 3.4	237 ± 2.1	195 ± 2.2	157 ± 3.5
H_C	1.014	0.933	0.670	0.998	1.093	0.842	0.571
μ_i	69.87	90.70	100.68	76.15	114.80	134.79	148.31

Figure 6 shows coercivity and permeability plotted against Vickers hardness. Although the absolute values are not the same (see Table 2), the trends in the data are similar, with an increase in coercivity and a corresponding decrease in initial permeabillity with increasing magnetic and mechanical hardness. These results indicate that the deployabe system could be used on tubes in-service to assess levels of degradation or for sorting mis-heat-treated/mis-manufactured grade 91 steel tube/pipes from the correctly heat treated service-entry ones.

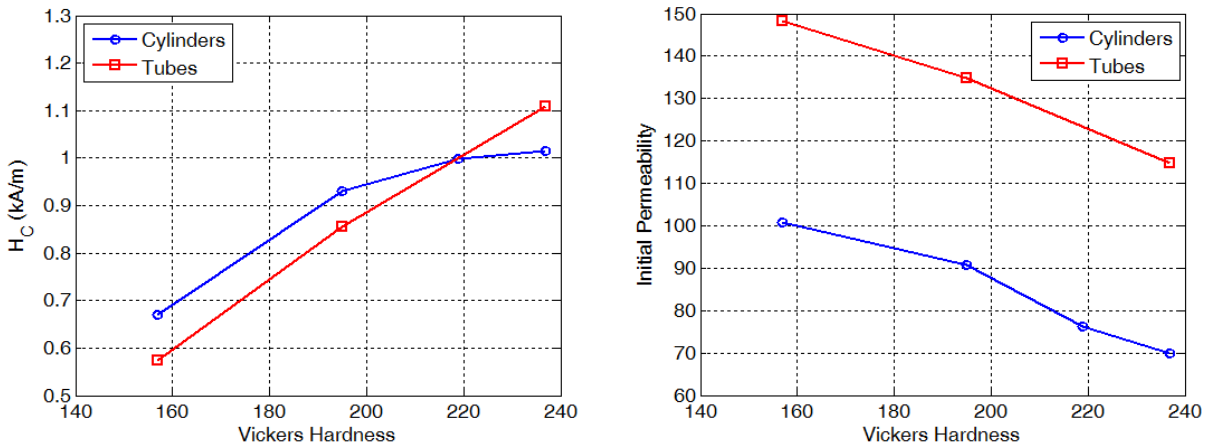

(a) **(b)**

Figure 6. a) Coercivity with respect to Vickers hardness, b) Initial permeability with respect to Vickers hardness

Acknowledgements

This work was carried out with financial support from the EPSRC under grant EP/H022937/1. The authors would like to thank EPRI for sample provision and David Allen at E.ON for providing the mis-heat treatment procedure and industrial furnaces for the heat treatments of the demonstration tube samples.

References

1. J F Henry, 'Growing experience with P91/T91 forcing essential code changes', Combined Cycle Journal, First Quarter 2005, pp. 8-17, 2005.
2. C Maharaj, J P Dear and A Morris, 'A Review of Methods to Estimate Creep Damage in Low-Alloy Steel Power Station Steam Pipes', Strain, Vol 45, No4, pp 316-331, August 2009.
3. G Sposito, C Ward, P Cawley, P B Nagy and C Scruby, 'A review of non-destructive techniques for the detection of creep damage in power plant steels', NDT & E International, Vol 43, Issue 7, pp 555–567, October 2010.
4. J Liu, X J Hao, L Zhou, M Strangwood, C L Davis and A J Peyton, 'Measurement of microstructure changes in 9Cr–1Mo and 2.25Cr–1Mo steels using an electromagnetic sensor', Scripta Materialia, Vol 66, Issue 6, pp 367–370, March 2012.
5. W Yin, N Karimian, J Liu, X J Hao, L Zhou, A J Peyton, M Strangwood and C L Davis, 'Measurement of electromagnetic properties of power station steels', NDT & E Int. Vol 51, pp 135-14, October 2012.
6. J W Wilson, G Y Tian, V Moorthy and B A Shaw, 'Magneto-acoustic emission and magnetic Barkhausen emission for case depth measurement in En36 gear steel', IEEE Trans. Magn. Vol 45, No 1, pp 177-183, January 2009.
7. G Bertotti, 1998 Hysteresis in magnetism: for physicists, materials scientists, and engineers (San Diego:Academic Press), ISBN: 0-12-093270-9.
8. H Kumar, J N Mohapatra, R K Roy, R Justin Joseyphus and A Mitra, 'Evaluation of tempering behaviour in modified 9Cr–1Mo steel by magnetic non-destructive techniques', Journal of Materials Processing Technology, Vol 210, No 4, pp 669-674, March 2010.
9. L Piotrowski, B Augustyniak, M Chmielewski, J Labanowski and M Lech-Grega, 'Study on the applicability of the measurements of magnetoelastic properties for a nondestructive evaluation of thermally induced microstructure changes in the P91 grade steel', NDT & E International, Vol 47, pp 157-162, April 2012.
10. A Hernando, P Crespo, P Marin, and A Gonzalez, Encyclopedia of Materials: Science and Technology, Magnetic Hysteresis, 2001, pp. 4780-4787.
11. D C Jiles, 'A self consistent generalized model for the calculation of minor loop excursions in the theory of hysteresis', Magnetics, IEEE Transactions on, Vol 28, No 5 pp 2602-2604, September 1992.
12. S Takahashi, S Kobayashi, H Kikuchi, and Y Kamada, 'Relationship between mechanical and magnetic properties in cold rolled low carbon steel', J. Appl. Phys. Vol 100, pp 113-908, December 2006.
13. V Moorthy, S Vaidyanathan, T Jayakumar and B Raj, 'On the influence of tempered microstructures on magnetic Barkhausen emission in ferritic steels', Philosophical Magazine A, Vol 77, No 6, pp 1499–1514, 1998.
14. O Saquet, J Chicois and A Vincent, 'Barkhausen noise from plain carbon steels: analysis of the influence of Microstructure', Materials Science and Engineering A, Vol 269, No 1, pp 73-82, 1999.
15. N Haned and M Missous, 'Nano-tesla magnetic field magnetometry using an InGaAs–AlGaAs–GaAs 2DEG Hall sensor', Sensors and Actuators A: Physical, Vol 102, No 3, pp. 216-222, 2003.
16. P K Heywood, 'Elevated Temperature Tensile Test and Microstructure / Hardness Examination of P91 Header Material: Results of tests on Materials 'As Supplied from the Mill' and after 'Anomalous Heat Treatment'', TEi Metallurgical Service, 2006, MS201B/06.

17. J Liu, J W Wilson, M Strangwood, C L Davis, A J Peyton and J Parker, 'Electromagnetic Evaluation of the Microstructure of Grade 91 Tubes/Pipes', International Journal of Pressure Vessels and Piping (submitted).